Electronic Supplementary Information (ESI)

Positively Charged Gold-Silver Nanostar Enabled Molecular Characterization of Cancer Associated Extracellular Vesicles

Yuan Liu, [a, b] *Wei Zhang,* [a, b] *Thanh Huyen Phan,* [c] *Wojciech Chrzanowski,* [c] *Alison Rodger* [b]

and Yuling Wang[*, a, b]

[a] ARC Center for Nanoscale BioPhotonics, Macquarie University, NSW, 2109, Australia

[b] Department of Molecular Sciences, Macquarie University, NSW, 2109, Australia

[c] School of Pharmacy, The University of Sydney, NSW, 2006, Australia

[*] Corresponding author: yuling.wang@mq.edu.au

TEM grids preparation

EVs were prepared for TEM measurement as follows: 50 μL EVs was mixed with 50 μL 2% (*w*/*v*) paraformaldehyde, and then a Cu grid was floating on this mixture drop for 20 min to absorb the EVs onto the grid which was then washed five-times with 10 mM phosphate buffered saline (PBS). Next, the Cu grid was placed onto a drop of 1% glutaraldehyde for 5 min, followed by another five-times washing with MilliQ water. Subsequently, the Cu grid was negatively stained by floating on a 2% uranyl acetate drop and waiting for 5 min. The grid was then dried at room temperature overnight.

Fluorescence emission/excitation

The emission spectrum of PANC1 EVs was averaged from 3 acquisition cycles with excitation at 280 and 296 nm with an excitation bandwidth of 1 nm. The excitation spectra were averaged from 3 measurements with excitation wavelength 335 nm with emission bandwidth of 5 nm.

AFM-IR measurements

1 μL PANC1 EVs sample was dropped onto a zinc selenide prism for overnight drying at room temperature in a desiccator. For the AFM observation, the above dried EV-loaded prism was placed onto the AFM scanning stage. Images were obtained at a scan rate of 0.5–0.8 Hz and the acquired scan size was 10 × 5 μm. For IR measurement on individual EVs, the cantilever tip was moved onto the EV of interest and kept in contact with it. The IR mode was switched on and the laser position was optimized before acquiring the nanoIR spectra. The IR spectrum was recorded under laser power of 35% with interval 4 cm^{-1} and a scan range from 1000–1800 cm^{-1}. Eleven individual EVs spectra were collected to acquire an averaged IR spectrum, which was further smoothed by Savitzky-Golay function in the Analysis Studio™ software.

Details of PCA-LDA procedure in SPSS

All spectra after background removal were firstly processed with the function "Factor Analysis" under the tag "Data Reduction" in SPSS. The generated principal components (PCs) were processed with "Nonparametric Test" under the tag "Analyze" to evaluate whether there is significant variation between groups. The PCs from the "Nonparametric Test" outcome with $p<0.05$ were considered as statistically significant and were input into the function "Discriminant Analysis" under the tag "Classify". The created report summarized the classification outcome, then the discriminate function and its score were used for plotting.

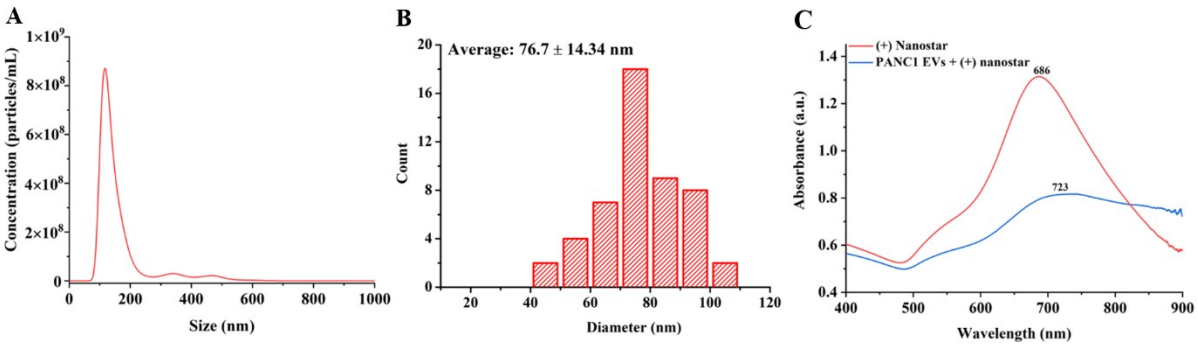

Figure S1. (A) Size distribution (nanoparticle tracking analysis, NTA) of PANC1 EVs isolated by ultracentrifuge. (B) size distribution (n=50) of nanostars from TEM measurements. (C) UV-Visible absorbance spectrum of nanostars and EV-nanostar complexes.

Table S1. Zeta potential of EVs and nanostar (Mean±SD, n=6).

Samples	Zeta potential (mV)
PANC1 EVs	-14.4±1.9
DU145 EVs	-24.6±0.8
SW480 EVs	-10.9±1.1

Positively charged nanostar	+27.7±1.2
Negatively charged nanostar	–31.0±0.5

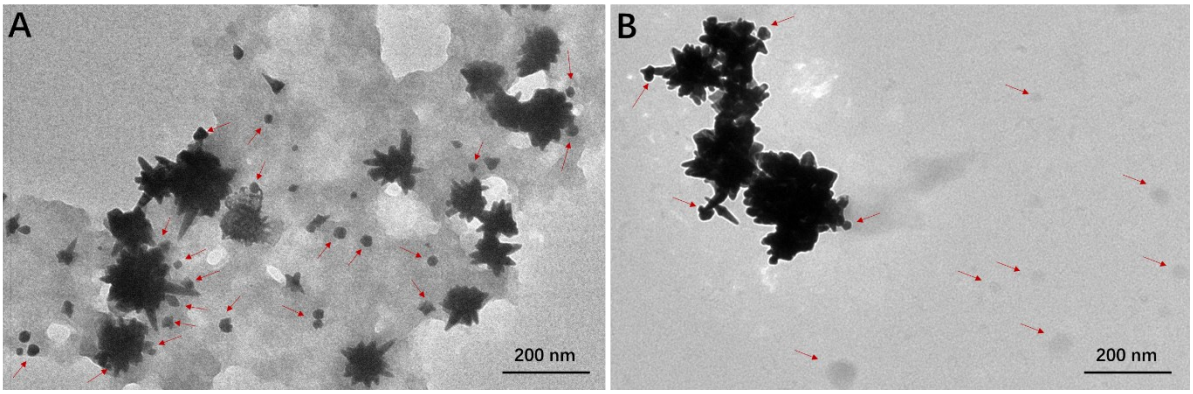

Figure S2. TEM images of the complex of (A) positively charged nanostar-PANC1 EVs and (B) negatively charged nanostar-PANC1 EVs. The ratio of nanostars and PANC1 EVs is 1.21.

Table S2. Possible peak assignment for SERS spectra of PANC1 EVs with nanostars. [1–5]

Raman shift (cm^{-1})	**Peak assignments**
667	N–type sugar pucker
729	Adenine
754	Symmetric breathing of tryptophan
786	Cytosine ring breathing mode, DNA backbone phosphodiester symmetric stretch
948	C–C–N stretching (*e.g.* α-helix backbone in protein)
1003	Amino acid
1295	CH_2 deformation (e.g., lipids)
1334	Ring breathing of adenine
1381	C=O symmetric stretching, CH_2 deformation, N–H in plane deformation (*e.g.* protein)
1449	CH_2, CH_3 deformation (*e.g.* protein backbone, acyl chain in lipids)

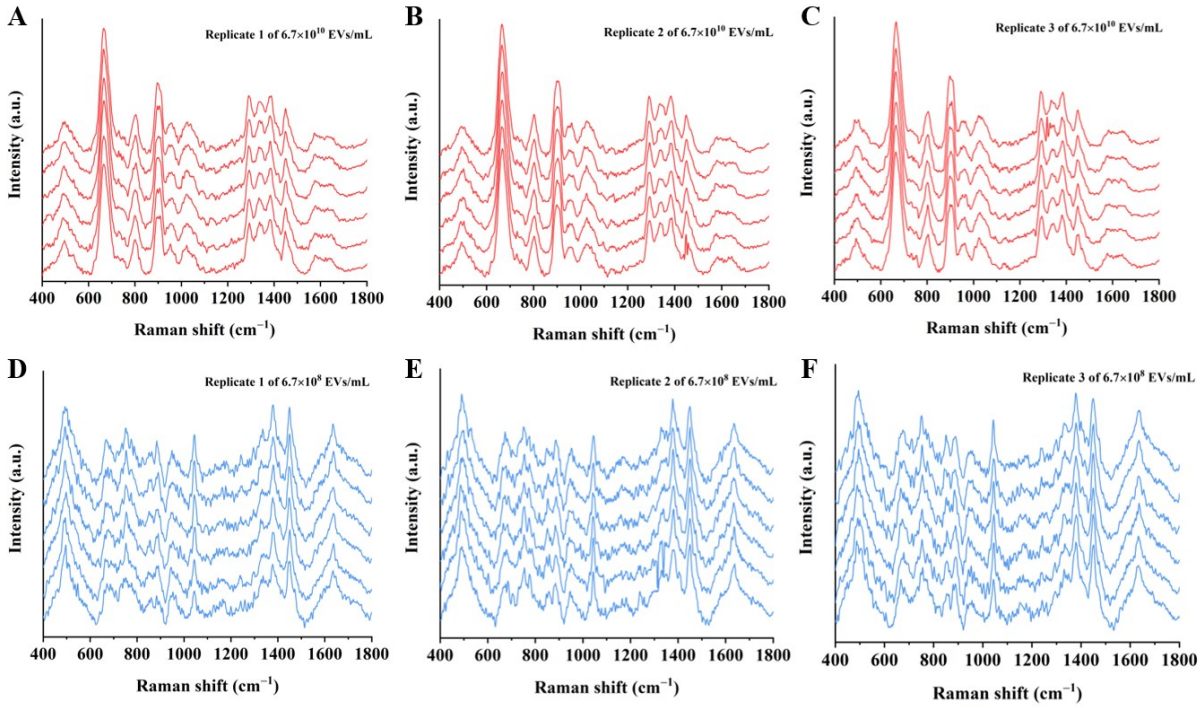

Figure S3. SERS spectra (after background removal) of PANC1 EVs from three technical replicates at (A–C) 6.7×10^{10} EVs/mL and (D–F) 6.7×10^{8} EVs/mL. Each replicate contains six individual measurements.

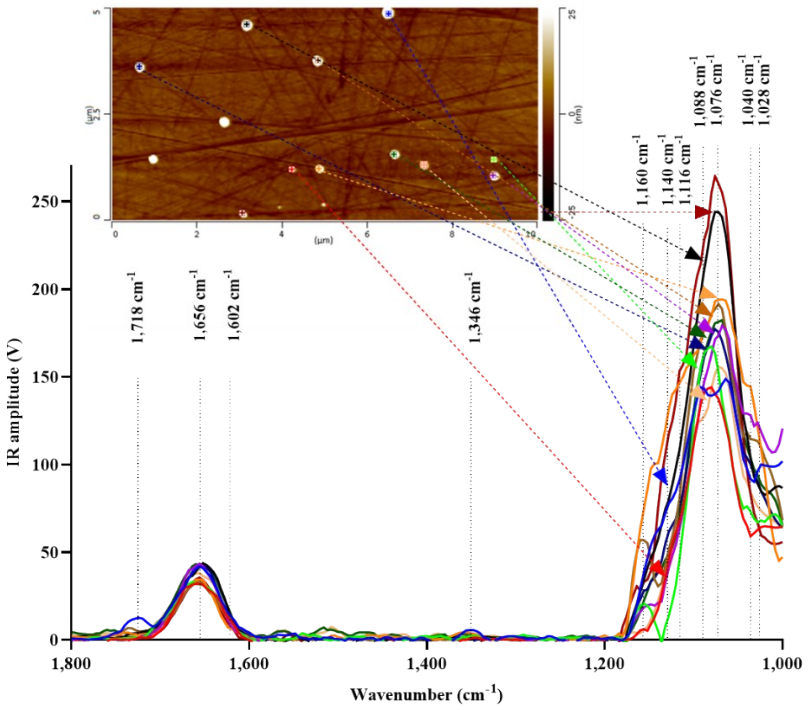

Figure S4. Two-dimensional AFM image and corresponding AFM-IR spectra for 11 individual PANC1 EVs isolated by ultracentrifuge.

Calculation of the ratio between nanostars and EVs in a laser spot

To better understand the ratio between the number of nanostars and EVs in the SERS measurements, the following calculation was performed and shows an approximate ratio of 55:1 at 6.7×10^8 EVs/mL.

The diameter (*d*) of the laser spot in liquid is 40 μm, pathlength (*h*) is 10 mm.

The volume of laser spot in liquid can be calculated as approximately:

$$V_{Laser\ spot} = \pi\left(\frac{d}{2}\right)^2 \times h$$
$$= \pi\ (20\ \mu m)^2 \times 10\ mm$$
$$= 1.3 \times 10^{-5}\ cm^3$$

For a SERS measurement, EVs (10 μL 6.7×10^8 EV/mL) were mixed with nanostar (60 μL). Hence, the final concentration of EVs in the mixture is calculated as:

$$C_{EVs\ in\ mixture} = \frac{C_{EVs} \times 10\ \mu L}{60\ \mu L + 10\ \mu L} = \frac{6.7 \times 10^8\ EVs/mL \times 10\ \mu L}{60\ \mu L + 10\ \mu L} = 9.6 \times 10^7\ EVs/mL$$

$$N_{EVs\ in\ laser\ spot} = C_{EVs\ in\ mixture} \times V_{Laser\ spot} = 9.6 \times 10^7 EVs/mL \times 1.3 \times 10$$

We assume that all the Au^{3+} (360 μL 10 mmol/L) has been reduced into nanostars:

$$Mole\ of\ Au^{3+} = 10\ mmol/L \times 360\ \mu L = 0.01\ mol/L \times 3.6 \times 10^{-4} L = 3.6 \times 10^{-6}\ mol$$
$$Mass\ of\ Au^{3+} = Mole_{Au^{3+}} \times Mw_{Au} = 3.6 \times 10^{-6}\ mol \times 196.97\ g/mol = 7.1 \times 10^{-4} g$$

$$V_{single\ nanostar} = \frac{4}{3}\pi r^3 = \frac{4}{3}\pi(53\ nm)^3 = 62000\ nm^3 = 6.2 \times 10^{-16} cm^3$$

where 53 nm is the radius of a nanostar.

$$Mass\ of\ single\ nanostar = \rho_{Au} \times V_{nanostar}$$
$$= 19.32\ g/cm^3 \times 6.2 \times 10^{-16} cm^3$$
$$= 1.2 \times 10^{-14} g$$

$$N_{total\ nanostar} = \frac{m_{Au^{3+}}}{m_{nanostar}} = \frac{7.1 \times 10^{-4}\ g}{1.2 \times 10^{-14}\ g} = 6.0 \times 10^{10}\ nanostars$$

$$C_{nanostar} = \frac{N_{total\ nanostar}}{10\ mL}$$

$$= \frac{6.0 \times 10^{10}\ nanostars}{10\ mL}$$

$$= 6.0 \times 10^{9} nanostars/cm^{3}$$

$$C_{nanostar\ in\ mixture} = \frac{C_{nanostar} \times 60\ \mu L}{60\ \mu L + 10\ \mu L} = \frac{6.0 \times 10^{9}\ nanostars/mL \times 60\ \mu L}{60\ \mu L + 10\ \mu L} = 5$$

$$N_{nanostars\ in\ laser\ spot} = C_{nanostar} \times V_{Laser\ spot}$$

$$= 5.1 \times 10^{9}\ nanostars/cm^{3} \times 1.3 \times 10^{-5} cm^{3}$$

$$= 66000\ nanostars$$

$$Ratio\ of nanostars/EVs\ in\ laser\ spot = \frac{66000\ nanostars}{1200\ EVs} = 55$$

Sensitivity, specificity, accuracy and receiver operating characteristic (ROC) curve of PCA-LDA classification for different EVs

Based on the PCA-LDA outcomes of three EVs (**Figure 3**), the sensitivity, specificity, and accuracy of the classification were calculated as follows:

sensitivity = true positive/(true positive + false negative)×100,

specificity=true negative/(false positive + true negative)×100,

accuracy = (true positive + true negative)/(true positive + false positive + false negative + true negative)×100.

Since all samples were correctly classified, the sensitivity is 100%, the specificity is 100% and the accuracy is 100%. The receiver operating characteristic (ROC) curve (*n*=90) of the PCA-LDA classification is displayed in **Figure S5**. It shows an area under curve is 1, illustrating this model has a good classification effect.

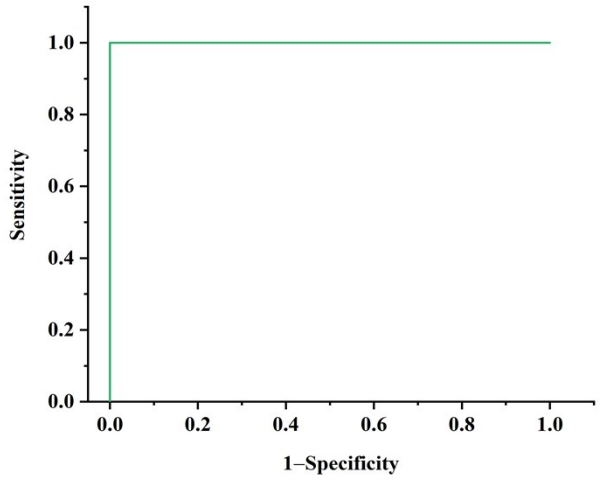

Figure S5. ROC curve of PCA-LDA classification on different EVs.

Table S3. Size distribution and concentration of EVs measured by NTA (Mean±SD, *n*=3).

Sample		Size (nm)	Concentration (particles/mL)
PANC1 EVs		$(1.1\pm0.1)\times10^{2}$	$(6.7\pm0.9)\times10^{10}$
DU145 EVs	Ultracentrifuge	$(1.2\pm0.3)\times10^{2}$	$(4.3\pm0.5)\times10^{11}$
SW480 EVs		$(1.2\pm0.1)\times10^{2}$	$(2.2\pm0.1)\times10^{11}$
PANC1 EVs		$(1.1\pm0.1)\times10^{2}$	$(9.8\pm0.9)\times10^{11}$
DU145 EVs	Kit	$(1.0\pm0.1)\times10^{2}$	$(1.4\pm0.2)\times10^{10}$
SW480 EVs		$(1.2\pm0.1)\times10^{2}$	$(2.7\pm0.6)\times10^{10}$
PANC1 EVs		$(1.3\pm0.1)\times10^{2}$	$(1.0\pm0.1)\times10^{10}$
DU145 EVs	SEC	$(1.2\pm0.1)\times10^{2}$	$(8.6\pm2)\times10^{9}$
SW480 EVs		$(1.2\pm0.1)\times10^{2}$	$(4.3\pm0.7)\times10^{9}$
	Batch 1	$(1.1\pm0.1)\times10^{2}$	$(2.0\pm0.1)\times10^{10}$
PANC1 EVs	Batch 2	$(1.2\pm0.1)\times10^{2}$	$(1.0\pm0.3)\times10^{10}$
	Batch 3	$(1.3\pm0.1)\times10^{2}$	$(1.4\pm0.7)\times10^{10}$
	Batch 1	$(0.8\pm0.1)\times10^{2}$	$(2.1\pm0.1)\times10^{11}$
DU145 EVs	Batch 2	$(1.0\pm0.1)\times10^{2}$	$(8.6\pm2)\times10^{10}$
	Batch 3	$(1.0\pm0.1)\times10^{2}$	$(1.7\pm0.3)\times10^{11}$
	Batch 1	$(0.9\pm0.1)\times10^{2}$	$(4.1\pm0.1)\times10^{10}$
SW480 EVs	Batch 2	$(1.1\pm0.1)\times10^{2}$	$(5.3\pm0.2)\times10^{10}$
	Batch 3	$(1.2\pm0.1)\times10^{2}$	$(4.0\pm0.2)\times10^{10}$

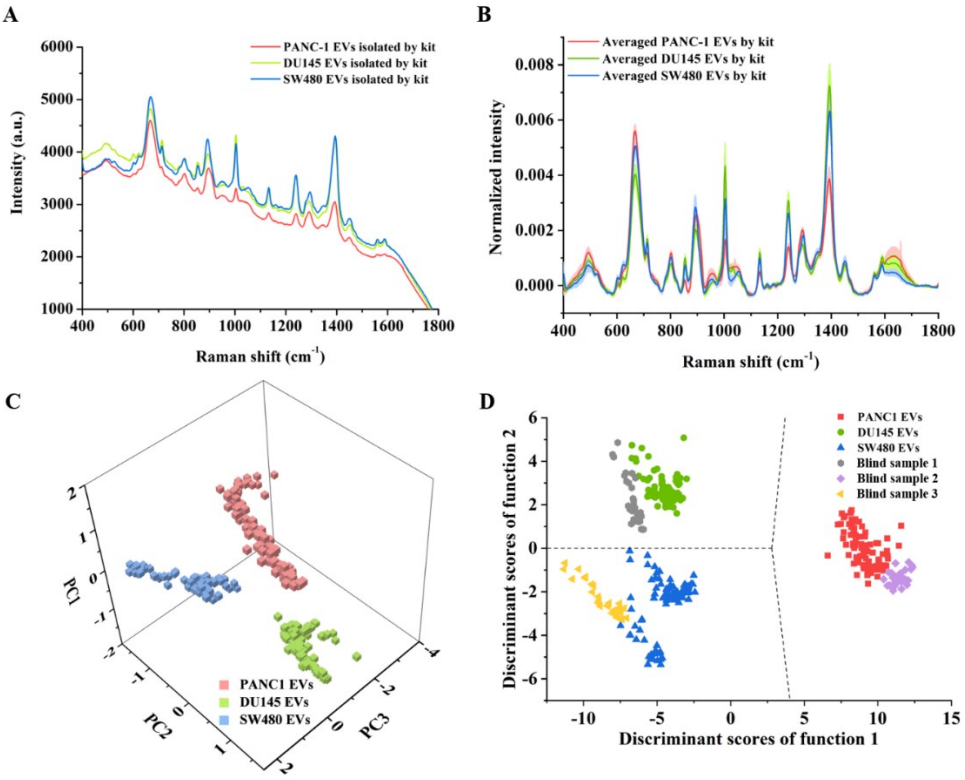

Figure S6. SERS spectra of PANC1 EVs, DU145 EVs and SW480 EVs (isolated by kit) (A) before and (B) after background removal. (C) 3D scattering map of the PCA results for EVs from three cell lines. (D) Discriminant LDA scores and the classification results for blind samples.

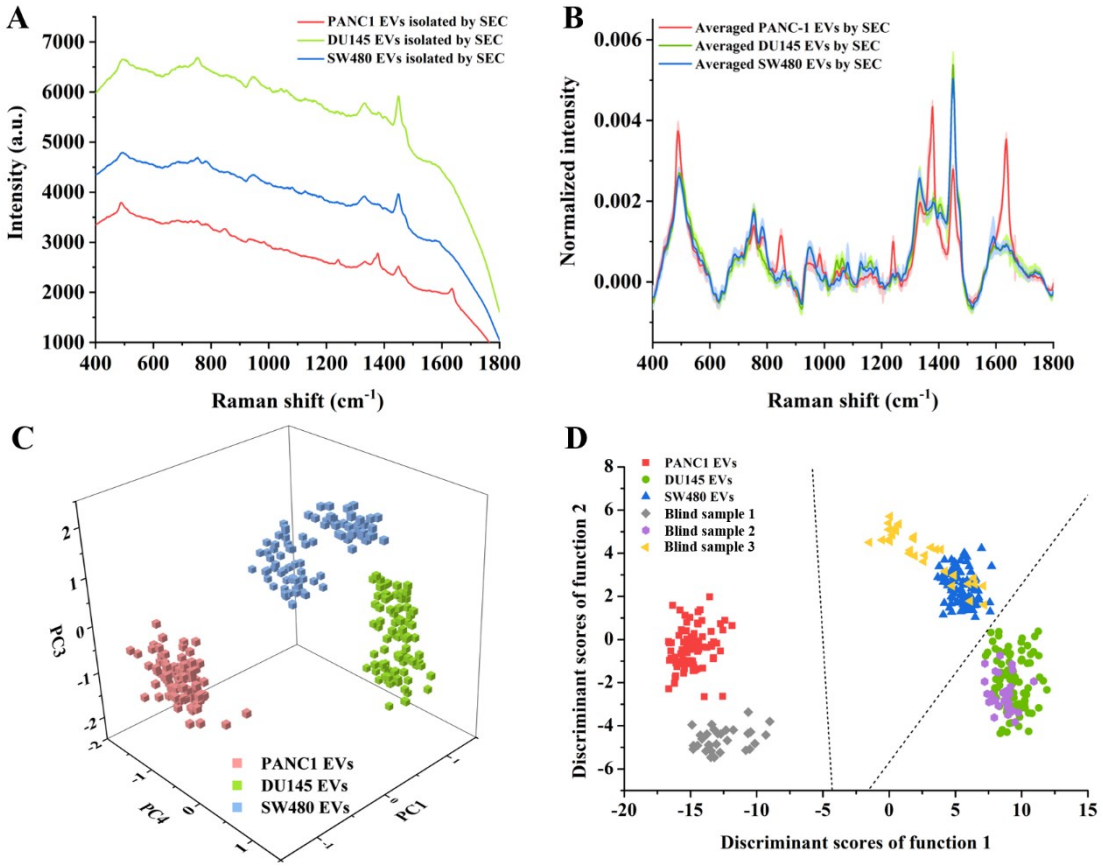

Figure S7. SERS spectra of PANC1 EVs, DU145 EVs and SW480 EVs (isolated by SEC) (A) before and (B) after background removal. (C) 3D scattering map of the PCA results for EVs from three cell lines. (D) Discriminant LDA scores and the classification results for blind samples.

References

1. J. Wang, K. M. Koo, E. J. Wee, Y. Wang and M. Trau, *Nanoscale*, 2017, **9**, 3496-3503.
2. X. Zhang, F. Yu, J. Li, D. Song, H. Li, K. Wang, Q. He and S. Wang, *Molecules*, 2019, **24**, 2059-2068.
3. W. W. Zheng, W. Huang, J. X. Chen, J. Q. Zhou, X. Xu, G. Xu, R. Y. Chen, G. W. Wang and S. Zhang, *Int. J. Clin. Exp. Med.*, 2018, 11, 12991-13002.
4. J. W. Chan, D. S. Taylor, T. Zwerdling, S. M. Lane, K. Ihara and T. Huser, *Biophys. J.*, 2006, **90**, 648-656.
5. A. C. S. Talari, Z. Movasaghi, S. Rehman and I. Rehman, *Applied Spectroscopy Reviews*, 2014, **50**, 46-111.